© 2019. Published by The Company of Biologists Ltd | Journal of Experimental Biology (2019) 222, jeb159277. doi:10.1242/jeb.159277

RESEARCH ARTICLE

The locomotor kinematics and ground reaction forces of walking giraffes

Christopher Basu*, Alan M. Wilson and John R. Hutchinson

ABSTRACT

Giraffes (*Giraffa camelopardalis*) possess specialised anatomy. Their disproportionately elongate limbs and neck confer recognised feeding advantages, but little is known about how their morphology affects locomotor function. In this study, we examined the stride parameters and ground reaction forces from three adult giraffes in a zoological park, across a range of walking speeds. The patterns of GRFs during walking indicate that giraffes, similar to other mammalian quadrupeds, maintain a forelimb-biased weight distribution. The angular excursion of the neck has functional links with locomotor dynamics in giraffes, and was exaggerated at faster speeds. The horizontal accelerations of the neck and trunk were out of phase compared with the vertical accelerations, which were intermediate between in and out of phase. Despite possessing specialised morphology, giraffes' stride parameters were broadly predicted from dynamic similarity, facilitating the use of other quadrupedal locomotion models to generate testable hypotheses in giraffes.

KEY WORDS: Locomotion, Quadruped, Dynamic similarity, Neck, Walk, Cursorial

INTRODUCTION

Giraffes, *Giraffa camelopardalis* (Linnaeus 1758), represent an extreme of many biological variables. They are the tallest living animal and the heaviest ruminant mammal. Whilst their extreme height confers a documented feeding advantage (Cameron and du Toit, 2007), the combination of disproportionately long neck and limb length with large body mass is also of consequence to other common behaviours, such as locomotion. For example, do giraffes' disproportionately long legs permit them to use relatively long stride lengths at a given speed? Does the mass of the head and neck cranially displace the centre of mass (COM) when compared with other cursorial quadrupeds? Beyond the influential work of Dagg (Dagg and Vos, 1968a,b; Dagg, 1962) and Alexander et al. (1977), giraffe gait dynamics remain seldom studied. In particular, there is no comprehensive examination of giraffe ground reaction forces (GRFs; but see Warner et al., 2013, which includes a giraffe GRF as part of an interspecific comparative dataset).

The focus of this study was to (1) quantify the basic kinematics and GRFs of the giraffe walking gait, (2) assess whether these gait parameters are speed dependent, (3) quantify the angular kinematics of the neck, and (4) question whether giraffes' walking gait parameters diverge from the trends predicted from other mammalian quadrupeds. In this study, we analysed such data from giraffes as they walked through an experimental setup in a zoological park.

Walking is giraffes' dominant locomotor behaviour, as the majority of their daily routine is spent foraging (Innis, 1958). The terminology used to describe the walking gait varies. Giraffes' walk has been referred to as a pace, a walking pace, a rack and an ambling walk (Bennett, 2001; Dagg, 1962; Innis, 1958; Kar et al., 2003). The use of differing terminology implies that giraffes' walking gait is specialised when compared with that of other mammalian quadrupeds, but this has not been tested.

A useful method for examining symmetrical gaits, where footfalls of the left and right side of the body are evenly spaced through time, is to quantify duty factor (the proportion of the stride that a foot contacts the ground, Eqn 1) and limb phase [the fraction of the stride between the forelimb (FL) footfall, relative to the ipsilateral hindlimb (HL) footfall, Eqn 2]. Using these two dimensionless numbers, symmetrical gaits may be compared at the level of the individual or species (Hildebrand, 1976):

$$\text{Duty factor} = \frac{\text{stance duration}}{\text{stride duration}}, \quad (1)$$

$$\text{Limb phase} = \frac{\text{Time}_{\text{FL foot-on event}} - \text{Time}_{\text{HL foot-on event}}}{\text{stride duration}}. \quad (2)$$

Giraffes use lower stride frequencies (and consequently longer stride lengths) at running speeds compared with other African ungulates (Alexander et al., 1977), a strategy which may be facilitated by their elongate limbs. It is unclear whether a similar strategy is employed at walking speeds. An expansion of this point is to question whether the unusual morphology of giraffes might have shifted their locomotor dynamics away from the general patterns predicted for walking quadrupedal mammals. The dynamic similarity hypothesis provides a useful framework for addressing this question. The principle of this theory assumes that subjects are geometrically similar to each other (Alexander and Jayes, 1983). In their study, Alexander and Jayes (1983) demonstrated that the broad trend in body shape versus mass is isometric (see their table 1), although noted that giraffes may be an 'extreme example' of how some quadrupedal mammals are not geometrically similar (e.g. they state that giraffes 'have twice the shoulder height of rhinoceros of equal mass'). In light of this, it remains uncertain whether giraffes' geometric dissimilarity is also associated with dynamic dissimilarity – in which case locomotor dynamics should diverge from those of other quadrupeds.

Stride parameters often vary as a function of speed. Stride duration, stance duration and duty factor typically vary inversely with speed, as demonstrated by a wide range of terrestrial animals (Hutchinson et al., 2006; Walker et al., 2010; Pfau et al., 2011; Shine et al., 2015; Gatesy and Biewener, 1991), including a study of an adult giraffe (Dagg, 1962). Studying how giraffes' stride and force parameters change with speed gives mechanistic insight into

Structure & Motion Laboratory, Royal Veterinary College, Hawkshead Lane, North Mymms, Hatfield, Herts AL9 7TA, UK.

*Author for correspondence (christopherbasu@gmail.com)

C.B., 0000-0002-2357-9516; J.R.H., 0000-0002-6767-7038

Received 10 March 2017; Accepted 7 November 2018

Journal of Experimental Biology (2019) 222, jeb159277. doi:10.1242/jeb.159277

List of symbols and abbreviations

a_1, a_2, a_3	Fourier coefficients
BM	body mass (kg)
BW	body weight (N)
COM	centre of mass
Fr	Froude number
g	magnitude of the acceleration due to gravity (m s^{-2})
GRF	ground reaction force (N)
h	shoulder height (m)
OLS	ordinary least squares
PPE	percentage prediction error (%)
ROM	range of motion
RMSE	root mean square error
T_{stance}	stance duration (s)
u	speed (m s^{-1})
ω	angular frequency (rad s^{-1})

how different speeds are attained, and whether giraffes' derived anatomy facilitates higher walking speed. Lameness is a welfare issue for giraffes in zoological collections (Hummel, 2006), so an understanding of giraffe gait at varying speed brings us closer to quantifying gait pathology.

The distribution of vertical impulse (the integral of vertical force throughout the stride duration) is unequal in most quadrupeds studied, with the forelimbs bearing a larger proportion of body weight than the hindlimbs (Alexander et al., 1979; Griffin et al., 2004; Hudson et al., 2012; Lee et al., 1999; Shine et al., 2015; Witte et al., 2004). This contrasts with most primates, which maintain a hindquarter-biased weight distribution (Raichlen et al., 2009). One explanation for a forequarter-biased distribution is that it is related to the mass of the head and neck. Indeed, disproportionate increases of these masses may lead to a cranial shift of the COM relative to foot position (Bates et al., 2016).

The role of the head and neck in quadrupedal locomotion is less frequently studied. In an adult giraffe, the mass of the head and neck accounts for approximately 10% of body mass (Mitchell et al., 2013; Simmons and Scheepers, 1996). This is similar to the proportion seen in the horse (Buchner et al., 1997), but in giraffes this mass is distributed over a longer distance, and the neck is carried with a more vertical posture (Dagg, 1962; Loscher et al., 2016).

In one comparative study of ungulate neck motion (Loscher et al., 2016), the majority of walking ungulates exhibited cyclical vertical neck acceleration which was out of phase with vertical trunk acceleration. This phase relationship probably results in net kinetic energy savings and potential metabolic savings. In giraffes, the vertical phase relationship was notably modest in comparison with the corresponding phase relationship observed in other ungulates, implying that mechanical energy conservation in the vertical plane is similarly modest. The horizontal phase relationship between neck and trunk acceleration was not studied, so it is as yet unclear whether neck motion in the horizontal plane contributes to or reduces COM acceleration.

Our aims for this study were: first, to identify the footfall patterns used by giraffes during walking; second, to quantify the stride parameters and GRFs of giraffes' walking gait and assess how these change with speed; third, to measure the angular kinematics of the neck across multiple strides; and finally, to assess to what degree giraffes conform to the predictions of dynamic similarity (and if applicable, in what ways they do not).

We specifically questioned whether or not giraffes use a true pacing gait, where a pace is defined with a limb phase <6.25% (Pfau et al., 2011); whether giraffes increase stride length over frequency to achieve faster walking speeds; and how neck excursion relates to gait parameters. We then quantified the percentage prediction error (PPE) associated with the predictions of dynamic similarity for giraffes.

MATERIALS AND METHODS

Animals

We collected synchronised video and force plate data from three adult reticulated giraffes (Table 1) kept at a zoological institution (Whipsnade Zoo, Bedfordshire, UK). The use of skin markers was not possible, as the animals were not accustomed to this type of manual handling. The giraffes were deemed as fit to participate by zoo veterinary staff. Giraffe 3 had a history of overgrown hoofs on both forefeet, but no sign of lameness was detected by veterinary staff throughout the course of the study, and the data were screened for potential subject effects (see 'Statistical modelling', below). This work was conducted with ethical approval from the Royal Veterinary College, University of London; Clinical Research Ethical Review Board number URN 2016 1538.

Data collection

We mounted a 6.0×0.9 m array of 10 AMTI three-axis force plates (Advanced Mechanical Technology, Watertown, MA, USA) with Hall-effect sensors onto a custom-built steel rack, into the giraffes' sand-covered outdoor enclosure. The rack was buried 5 cm below the substrate surface and covered with sand; this was necessary to allow the giraffes to display normal locomotor behaviour and to prevent inadvertent excavation around the edges of the rack. The array was positioned along a fence, with enough room at either end for giraffes to accelerate or decelerate prior to walking over the force plates (Fig. 1).

The animal keepers led the giraffes back and forth across the force plate array, motivating the animals by carrying foodstuffs ahead of them. Data were collected over the course of 1 h per day, for 6 days spread across two batches of data collection, separated by a period of 3 months. The keepers elicited a range of giraffe speeds by varying their own speed.

The voltage output of the force plates was recorded using an analog-to-digital data acquisition instrument (National Instruments, Newbury, Berkshire, UK) connected to a laptop. A manual trigger was used to start 30 s recordings of the force plate signals, at 240 Hz per channel. Data acquisition was controlled using a custom-written LabView (National Instruments) script.

Two Hero3+ cameras (GoPro, San Mateo, CA, USA) were mounted perpendicular to the fence. Camera 1 was aimed at the

Table 1. Giraffes used in data analysis, with a breakdown of their contributions to the dataset

					No. of trials		
Subject	Sex	Age (years)	Body mass (kg)	Shoulder height (m)	Forelimb GRF	Hindlimb GRF	Neck kinematics
1	M	3	800	1.84	4	1	3
2	F	7	750	1.87	8	7	10
3	F	14	780	1.87	34	21	33

GRF, ground reaction force.

Journal of Experimental Biology (2019) 222, jeb159277. doi:10.1242/jeb.159277

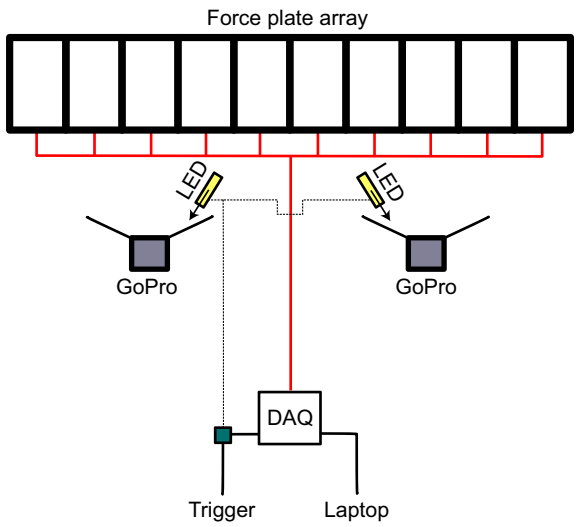

Fig. 1. Experimental setup. A wire fence ran parallel to the force plate array, in between the giraffes and equipment. Animal keepers led the giraffes back and forth (left and right) along the force plate array. Sufficient space was allowed for acceleration and deceleration. The remote trigger started 30 s of force plate data collection, as well as triggering the LED lights to mark the time on the video recordings. Raw force plate voltages were transduced by the data-acquisition device (DAQ). The GoPro cameras were situated at a perpendicular distance of 5 m from the force plate array.

centre of force plates 1–5, and camera 2 was aimed at force plates 6–10. Video data were collected at a frame rate of 120 Hz. The force plate trigger was also connected to an LED light, positioned to be in the field of view of both cameras, so that the start of the 30 s recordings could be synchronised to video. The study area was calibrated at the start of each day of data collection; a grid of known dimensions was walked through the space, allowing pixel distances in the digital videos to be converted to metres. Cameras subsequently were not moved. A repeat calibration to assess for inadvertent (e.g. wind-induced) movement was not performed after each data collection, as it was not possible to access the giraffe paddock once the giraffes were outdoors.

Data processing

The force plate signals were processed with custom-written Matlab (MathWorks, Natick, MA, USA) software, which took raw voltages and converted them to calibrated GRFs, using plate-specific calibration matrices. Calibrated forces were filtered using a zero-phase (back and forth) fourth-order Butterworth filter with a 6 Hz cut-off. A further custom-written script calculated peak forces and impulses.

The camera distortion was corrected using GoPro Studio 2.5. The cameras were calibrated using the grid of known dimensions as a reference, allowing each pixel in the field of view to be assigned a calibrated displacement from the image origin. The video data were digitized using DLTDV6 (Hedrick, 2008). To measure speed, neck angle and stride parameters, we devised a virtual marker system consisting of the coronary band of each foot, a point behind the ear, a point on the giraffe's withers and a point at the lumbosacral region (Fig. 2A). Each giraffe had a comparable virtual marker system which was adhered to throughout data processing.

Strides were defined as stance phase followed by swing phase. Stride parameters were measured from the near-side of the body with respect to the cameras during each trial. Foot contact times were determined using a consistent combination of force plate and video data. Stance duration, indicated by foot-on and foot-off events, was determined using the force/time derivative from force plate data, where a threshold of 1 N ms^{-1} was used to determine the timing of rapid loading and unloading associated with the stance phase. The subsequent foot-on event (indicating the end of the stride) was frequently not available from force plate data, because the giraffes commonly placed contralateral forelimbs and hindlimbs onto the same force plate, resulting in mixed GRF recordings. Instead, we used the digitised foot motion and a velocity threshold of 1 m s^{-1} to denote the end of the stride (Starke and Clayton, 2015). Stride length was calculated as the displacement of the foot between the start and end of the stride, and stance distance was defined as the displacement of the withers during the stance duration.

Speed was determined for each stride by calculating the mean velocity of the withers and lumbosacral points over the duration of the stride. Two digitised points were used to reduce the possibility of positional error. Speed was converted to Froude number (Fr) (Eqn 3), where u is speed (m s^{-1}), g is the magnitude of the acceleration due to gravity (9.81 m s^{-2}) and h is shoulder height (m), to allow comparisons between giraffes and other species (Alexander and Jayes, 1983):

$$Fr = \frac{u^2}{gh}. \quad (3)$$

We only included strides that featured steady-state locomotion. We measured the velocity of the withers and lumbosacral digital markers over 0.2 s during the start and end of the stride, and compared any difference with the overall speed. Strides with acceleration or deceleration over 20% of the overall speed were excluded from the analysis (Shine et al., 2015). The remaining strides were checked again for changes in speed, by calculating the goodness of fit of an ordinary least squares (OLS) linear model to the time series data for the withers marker. Any strides with R^2 values <97.5% were excluded from the analysis.

Body weight (BW; in N) was determined for each giraffe by calculating the time-averaged vertical impulse of an entire stride cycle, where all four feet made complete contact with the force plate array. Five measurements of BW per giraffe were used to calculate the mean values, which were subsequently used to standardise selected force parameters. Vertical, craniocaudal and mediolateral GRFs were included in the analysis. Peak forces were standardised by BW. In steady-state locomotion, the sum of the vertical impulses from all four feet can be defined as:

$$\sum \text{Impulse}_{\text{vert}} = \text{BW} \times \text{stride duration}. \quad (4)$$

This can be rearranged to:

$$\frac{\sum \text{Impulse}_{\text{vert}}}{\text{BW} \times \text{stride duration}} = 1. \quad (5)$$

We therefore further standardised $\text{Impulse}_{\text{vert}}$ to BW and stride duration. Craniocaudal impulses ($\text{Impulse}_{\text{CC}}$) were also standardised in the same manner. The GRFs recorded in the current study were from independent strides, as we did not obtain ipsilateral forelimb and hindlimb footfalls from the same stride. We estimated the relative contribution of forelimbs and hindlimbs to COM balance by separately modelling $\text{Impulse}_{\text{vert}}$ for the forelimbs and hindlimbs using OLS linear regression. By looking at the $\text{Impulse}_{\text{vert}}$ predictions at a given speed, the relative distribution of BW between the forelimbs and hindlimbs could be quantified.

Journal of Experimental Biology (2019) 222, jeb159277. doi:10.1242/jeb.159277

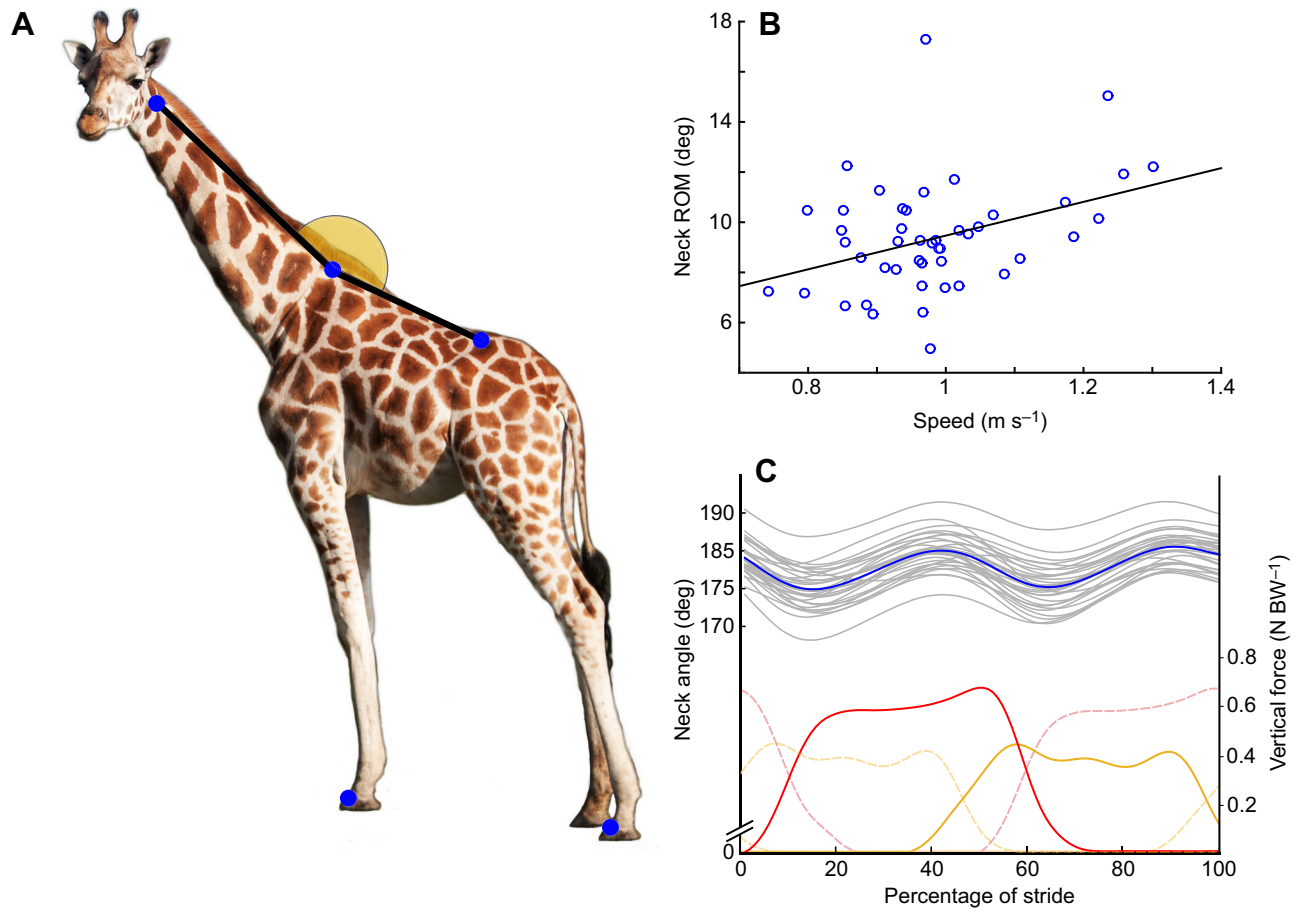

Fig. 2. Giraffes' neck kinematics during walking. (A) An adult giraffe showing the digital marker system (blue dots) and definition of neck angle. (B) Scatter plot of neck range of motion (ROM) versus speed. Linear regressions are shown as a black line in the form $y=au+b$ (see Table S2 for further details). Neck range of motion increased as a function of walking speed (y=6.4u+3.1, R^2=0.13, P=0.01; n=46). (C) Time series of the mean neck angle (blue line) and individual trials (grey lines) throughout one forelimb stride, with relative timing of mean forelimb and hindlimb ground reaction forces (GRFs) (red and yellow solid lines, respectively) and contralateral limb GRFs (dashed lines). The neck oscillated twice during each stride, with peak dorsiflexion occurring in the early stance of the left and right forelimb.

Fourier analysis

GRF components have previously been modelled using a Fourier analysis (Alexander and Jayes, 1980; Hubel and Usherwood, 2015), where the GRF_{vert} profile was represented by three sine wave coefficients of the form:

$$\frac{F_z}{mg} = a_1 \sin\left(\pi \frac{t}{T_{stance}}\right) + a_2 \sin\left(2\pi \frac{t}{T_{stance}}\right) + a_3 \sin\left(3\pi \frac{t}{T_{stance}}\right), \quad (6)$$

where F_z is vertical force and T_{stance} is stance duration. The three coefficients provide a means to quantitatively describe the shape of the force profile over the stance duration, and allow quantitative comparison with other GRF data. In Eqn 6, the coefficients dictate the magnitudes of different-shaped sine waves during T_{stance}; a_1 dictates the magnitude of a single-peaked positive sine wave, a_2 a positive followed by negative wave, and a_3 a doubled-peaked positive wave.

A Fourier series was fitted to representative GRF_{vert} data from the forelimb and hindlimb, by finding the solution that minimised the root mean square error (RMSE) between the experimental and fitted data in custom-written Matlab code. We used Fourier constants to model how the GRF_{vert} profile changed as a function of speed. The angular neck kinematics of the giraffe were also fitted to a Fourier series, to allow for future comparisons with other quadrupedal species.

Statistical modelling

Statistical procedures were carried out using the Matlab Statistical Toolbox. Variables were first assessed for normality using a Kolmogorov–Smirnov test. Any differences in the kinematic and kinetic parameters with regard to the forelimb versus hindlimb were first identified using an analysis of co-variance (ANCOVA), with stride and force parameters as the dependent variable, speed as the covariate, and forelimb or hindlimb as the independent variable. Differences between forelimb and hindlimb data in terms of regression slope and parameter mean (adjusted to compensate for speed variation) were tested as part of the ANCOVA. Data for the forelimb and hindlimb were subsequently treated separately if a significant difference was identified. To assess the significance of regression slopes, OLS linear regressions were subsequently performed using speed as the independent variable, and stride and force parameters as the dependent variable. To correct for the increase in Type 1 error rate associated with multiple statistical comparisons, we used the Benjamini–Hochberg procedure (Benjamini and Hochberg, 1995). This procedure reduces the probability of Type I error

Journal of Experimental Biology (2019) 222, jeb159277. doi:10.1242/jeb.159277

by cumulatively adjusting the critical values for null hypothesis rejection, up to a false discovery rate. We applied this correction to the ANCOVA and OLS regression comparisons, using a false discovery rate of 0.05.

The potential for inter-giraffe subject effects on stride and force parameters was separately assessed using mixed effect linear modelling. Stride length and peak force were each modelled as response variables, with speed as the predictor and giraffe identity as an additional fixed effect. The significance of giraffe identity in both stride length and peak force was tested by comparing models with and without the effect, using a likelihood ratio test.

RESULTS

Seventy-five strides featuring a complete GRF and associated kinematics were analysed, representing approximately 5% of the total dataset. The remaining strides were excluded on the grounds of having excessive acceleration or deceleration, obscured footfalls or incomplete GRFs.

As paired forelimb and hindlimb GRFs from the same stride could rarely be recorded, the GRF data used in the analysis are from isolated forelimb or hindlimb footfalls (Table 1). Parameter means and/or regression slopes were different between the forelimbs and hindlimbs (Table S1), aside from stride length, stride frequency and peak propulsive force. All parameters followed a normal distribution, and giraffe identity did not have a significant effect on stride length or peak force (likelihood ratio test, P=0.84 and P=0.97, respectively).

Kinematics

Despite the keepers' attempts to evoke a wide range of speeds, the giraffes elected to use a narrow speed range from 0.74 to 1.3 m s^{-1}, with a mean speed of 0.98 m s^{-1} (0.054 *Fr*), a combined mean duty factor of 0.70 and mean limb phase of 0.14. In conventional gait terminology (Hildebrand, 1989), this can be expressed as a 70:14 symmetrical gait, or a lateral sequence walk (Fig. 3).

All linear regressions are summarised in Table S2. Faster speeds were associated with marked increases in stride length (Fig. 4A) and subtle increases in stride frequency (the inverse of stride duration); for every 1 m s^{-1} increase in speed, stride length and frequency increased by a factor of 1.3 and 0.17, respectively. Stance duration decreased whilst swing duration was maintained across the speed range, accounting for the observed drop in duty factor and stride duration (Fig. 4B,C) with faster speeds. Mean duty factors were 1.07× greater in the forelimb than in the hindlimb (P<0.001; Table S1).

The neck oscillated twice during any given stride (Fig. 2C); peak dorsal extension occurred during each (left and right) early forelimb stance, with peak ventral flexion occurring in each forelimb mid-stance. The time series of neck angle for each trial was modelled using a two-term Fourier series with a mean RMSE of 0.074 deg (Table S3). The range of motion (ROM) of the neck during stance had a positive relationship with speed (P=0.015), indicating that the amplitude of neck ROM was greater at faster speeds (Fig. 2B).

GRFs

Forelimb and hindlimb GRF_{vert} profiles were comparable with the M-shaped profiles seen in other walking animals, but had some contrasting features (Fig. 5). In the forelimb, two GRF_{vert} profile shapes were observed. Giraffes 1 and 3 displayed shape F1, typified by a reduced early-stance peak, whilst giraffe 2 displayed type F2, consisting of two pronounced peaks (Fig. 5C,D). In each of the shapes, the late stance peak was typically higher than that in early stance. The two profiles were observed at similar speeds (mean of 0.05 and 0.06 *Fr*, respectively), so we do not attribute this variation in GRF_{vert} to a function of walking speed. Two distinct hindlimb GRF_{vert} profile shapes were also apparent (Fig. 5E,F), but this variation occurred both within and between individuals. Shape H1 had two peaks, whereas shape H2 had an additional third peak, occurring during mid-stance.

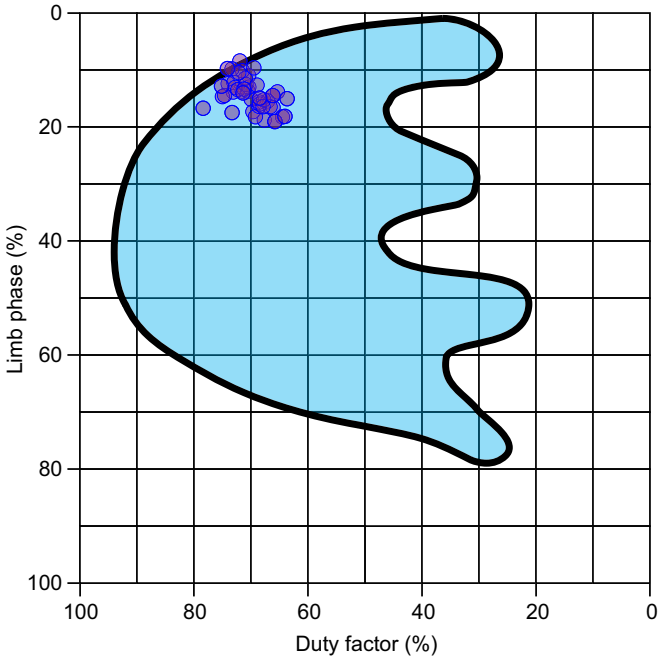

Fig. 3. Categorisation of giraffes' walking gait. Reproduction of Hildebrand's plot for symmetrical gaits of terrestrial vertebrates (Hildebrand, 1976), with overlying giraffe data from the current study. The mean duty factor and limb phase for walking giraffes were 0.7 and 0.14, respectively, and the majority of strides were within the continuum of previously observed symmetrical gaits. These data show that giraffes use a lateral sequence walk.

To quantitatively describe the shape of the GRF_{vert} profiles, representative data were fitted to a Fourier series. The resulting fits had low RMSEs (mean=0.06; Table S4), and the profiles were comparable with a Fourier analysis of human GRF_{vert} profiles (Hubel and Usherwood, 2015). The shape of the forelimb GRF_{vert} profiles, as modelled by Fourier coefficients, changed as a function of speed, with each coefficient increasing in magnitude (Fig. 6A). In contrast, there was no apparent relationship between hindlimb GRF_{vert} profile and speed (Fig. 6B).

Fourier modelling did not distinguish between the two observed hindlimb GRF_{vert} shapes. Adding extra Fourier terms up to the next odd harmonic further reduced the RMSE in both H1 and H2, but this did not discriminate between these shapes. Instead, the presence of a third (mid-stance) peak was established by qualitatively grouping the hindlimb GRF_{vert} profiles according to the presence or absence of a third peak, and testing (using a one-way ANOVA) whether this grouping had an effect on the difference between peak force at mid-stance and the overall peak force. The presence of a third peak was statistically distinguishable from background variation (ANOVA, P=0.003).

Peak vertical forces did not change significantly within the measured speed range (Fig. 7A), but were 1.9 times greater in the forelimbs. When standardised by BW and stride duration (Fig. 7B), forelimb and hindlimb $Impulse_{vert}$ did not change significantly with speed (P=0.269 and P=0.047, respectively). The sum of standardised forelimb and hindlimb $Impulse_{vert}$ should account for

Journal of Experimental Biology (2019) 222, jeb159277. doi:10.1242/jeb.159277

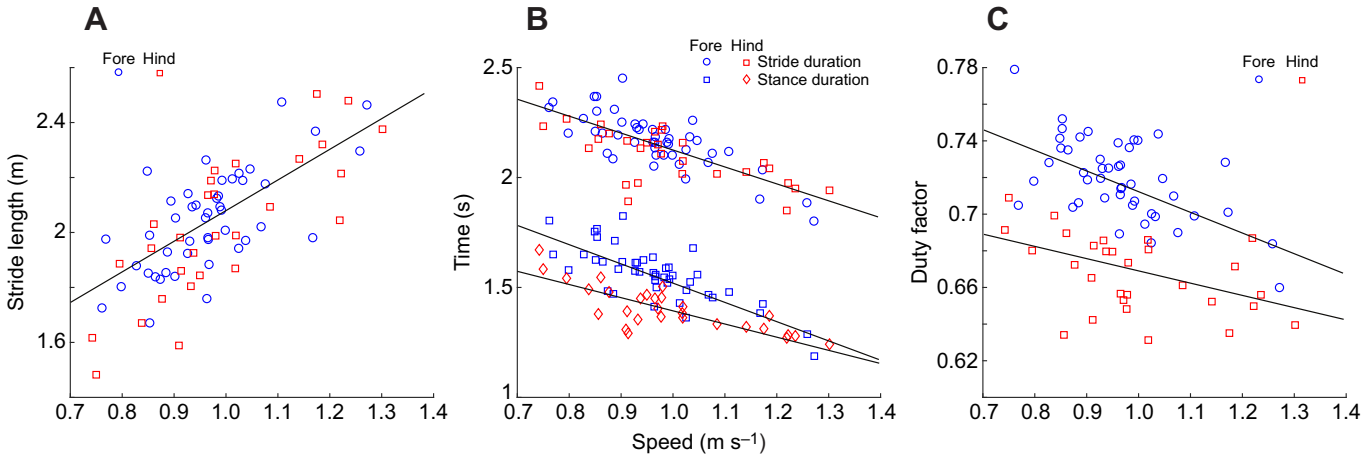

Fig. 4. Kinematic gait parameters in giraffes, as a function of speed. (A) Increases in speed were achieved through a marked increase in stride length (y=1.2u+0.8, R^2=0.54, P<0.01). (B) Stride duration (y=−0.75u+2.9, R^2=0.55, P<0.01) fell with speed. Stance duration was longer in the forelimb (y=−0.87u+2.4, R^2=0.6, P<0.01) than in the hindlimb (y=−0.55u+1.9, R^2=0.62, P<0.01), resulting in (C) a higher duty factor in the forelimb (y=−0.12u+0.83, R^2=0.36, P<0.01) than in the hindlimb (y=−0.07u+0.73, R^2=0.23, P<0.01).

50% of BW (the other half being accounted for by the contralateral limbs). The mean values here summed to 48% of BW, with a forelimb to hindlimb vertical force ratio of 65:35. The unaccounted 2% is attributed to measurement and statistical error; particularly because forelimb and hindlimb data were from separate strides. The measurement error can be demonstrated by the standard deviation of

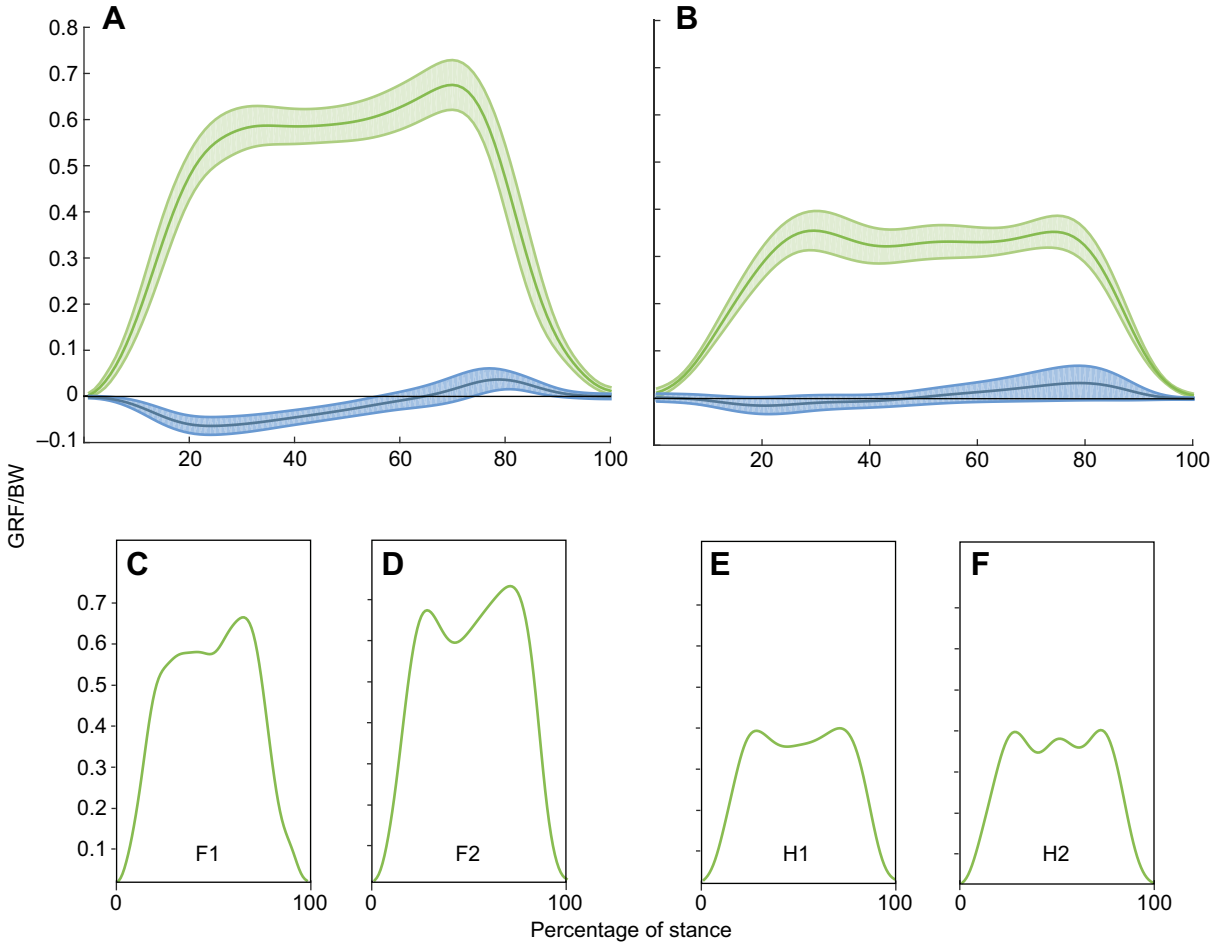

Fig. 5. Ground reaction forces in walking giraffes. (A) Forelimb GRFs were characterised by a double-peaked vertical GRF, with the second peak having a greater magnitude (n=46). (B) Hindlimb GRFs. Shaded areas represent ±1 s.d. (n=29). (C,D) Examples of inter-subject variation in the vertical GRF profiles (F1, F2) of the forelimb. (E,F) Examples of intra-subject variation in the vertical GRF of the hindlimb (H1, H2). The profiles in C–F were selected on the basis of their shape, and whether their associated speed was within 1 s.d. of the mean (to exclude extreme examples).

Journal of Experimental Biology (2019) 222, jeb159277. doi:10.1242/jeb.159277

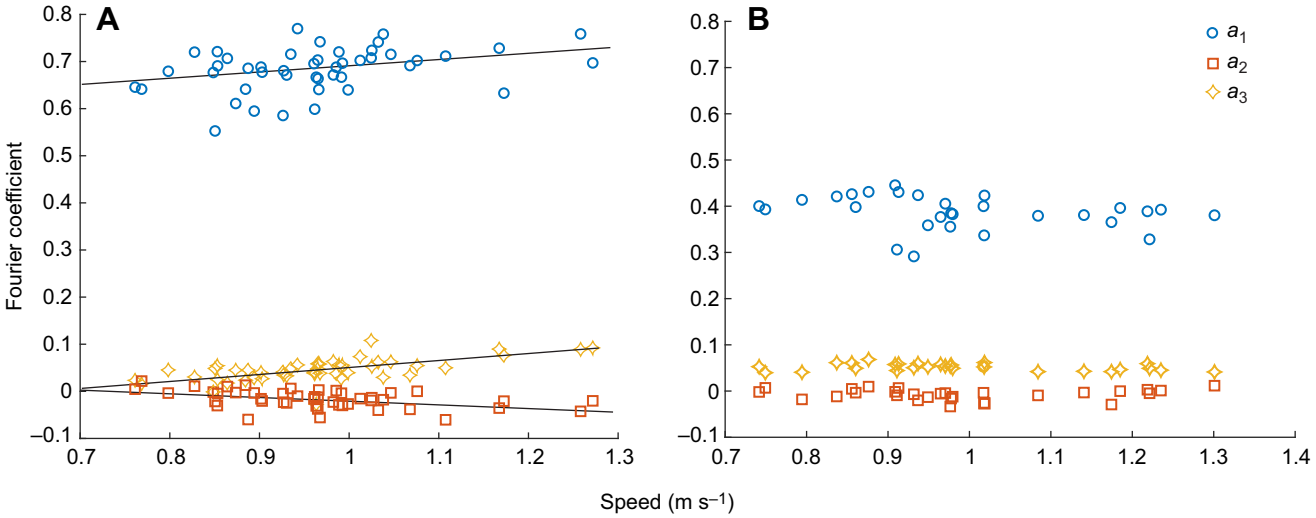

Fig. 6. Fourier modelling of GRFs. Fourier coefficients (a_1, a_2 and a_3) changed as a function of speed in the forelimb (A), leading to GRF shapes with exaggerated peaks during late-stance and lower mid-stance forces, but were constant in the hindlimb (B).

the repeated body mass measurements for each individual, which ranged from 1.3% to 1.6% of BW, whilst the statistical error was demonstrated by the RMSE seen in the forelimb and hindlimb linear models, which was 2% in both cases.

Craniocaudal ground reaction forces (GRF_{CC}) in the forelimbs and hindlimbs were characterised by negative (braking) forces in early stance, changing to positive (propulsive) forces in late stance (Fig. 5A,B). Peak braking force in the forelimb increased in magnitude with speed (P=0.003). The ANCOVA-adjusted mean net $Impulse_{CC}$ (standardised to BW and stride duration) was higher in the hindlimb versus the forelimb (0.006 and −0.002, respectively; ANCOVA, P=0.012; Table S1). Net $Impulse_{CC}$ was statistically indistinguishable from zero in the forelimb (t-test, P=0.2614), whilst being positive in the hindlimb (t-test, P=0.003). The ANCOVA-adjusted mean positive $Impulse_{CC}$ was equal in the forelimb and hindlimb (P=0.584). In contrast, the ANCOVA-adjusted mean negative $Impulse_{CC}$ was of greater magnitude in the FL (P<0.001; Table S1). Mediolateral forces were of low magnitude, accounting for 0.7% of the total impulse.

DISCUSSION

The giraffes in the current study used a lateral sequence walk, or in Hildebrand terms, a 70:14 gait (Fig. 3). This is a typical walking gait used by quadrupeds, and is different from a pacing gait, which can be seen in some running horses, dogs and camels (where limb phase is below 6.25%). Despite popular accounts that giraffes pace, at no point in this study did the limb phase reach a level consistent with this definition, similar to the confusion surrounding which footfall pattern alpacas use (Pfau et al., 2011).

The giraffes were able to achieve faster walking speeds whilst maintaining relatively conserved stride frequencies, illustrating that giraffes increase walking speed predominantly by taking longer strides. It is possible that the narrow range of observed stride frequencies in giraffes is close to their limbs' natural frequency. Assuming a pendulum model of walking, increases of stride frequency in excess of natural frequency are met with a sharp increase in force and work requirements. In humans, such increases are associated with corresponding increases in metabolic cost (Doke et al., 2005). Larger organisms such as giraffes may be particularly sensitive to this relationship, given their relatively large limb inertia.

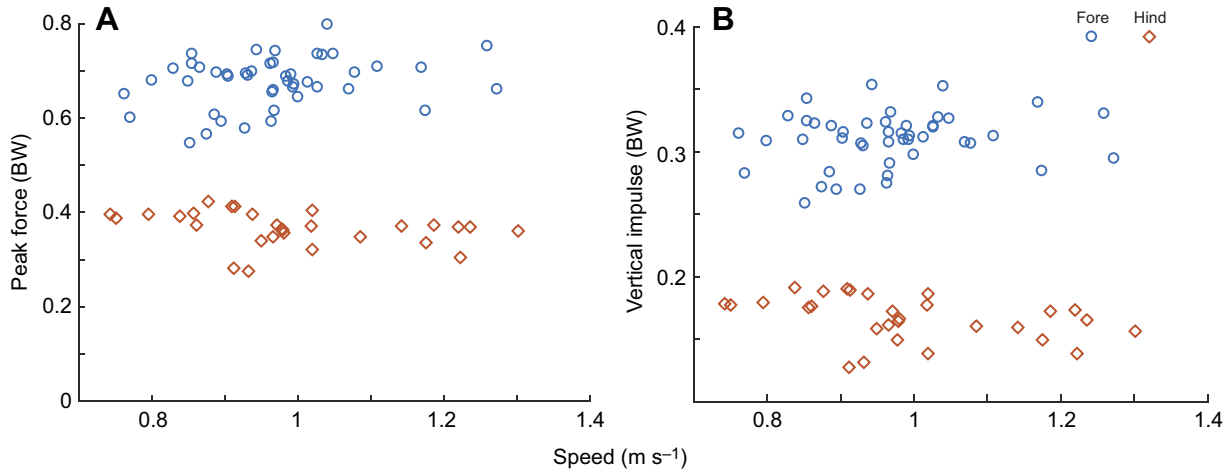

Fig. 7. Kinetic parameters as a function of speed. (A) Peak forces, standardised by body weight (BW) were higher in the forelimb versus hindlimb. In both cases, peak force was consistent across the observed range of speeds. (B) Vertical impulse, standardised by BW and stride duration, did not significantly change with speed in the forelimb (P=0.269) or hindlimb (P=0.047). The ratio of impulses indicated a forelimb:hindlimb weight distribution of 65:35.

Giraffes may preferentially select stride frequencies that are optimised for metabolic economy (Loscher et al., 2016).

Duty factors were consistently greater in the forelimb than in the hindlimb (Fig. 4C). The greater forelimb duty factors observed here offset the higher peak force experienced in the forelimb by spreading the impulse over a longer stance duration. If duty factors remain greater in the forelimb at near-maximal speed, they may have a role to play in maintaining tissue safety factors (Biewener, 1983).

Duty factor is causally related to peak force (Alexander et al., 1979; Witte et al., 2004). Each foot must support a proportion of the total BW over the course of a stride. As duty factor was lower at faster speeds, $\text{Impulse}_{\text{vert}}$ was compressed into shorter stance durations; therefore, we expected to see an increase in peak vertical force with speed. Yet, there was no significant change with speed (Fig. 7A). We have considered the presence of substrate as an unlikely explanation for this result. Compliant substrates are associated with dampening of the initial impact GRF, not peak mid-stance vertical force, when compared with firm substrate (Parkes and Witte, 2015). This relationship may explain the lack of an impact peak in the observed GRFs. Deep wet sand substrates are also associated with a reduction of peak mid-stance force, but this is associated with the lengthening of stance duration (Crevier-Denoix et al., 2010). We speculate that peak forces in giraffes are instead dampened by compliant musculotendon units. Giraffe tendons are long, and relatively slender (e.g. the digital flexor muscles), and it is reasonable to hypothesise that they have a high amount of compliance (Zajac, 1989). As compliant limbs are observed to dampen peak force (McMahon et al., 1987; Ren et al., 2010), giraffes may conserve peak force at a consistent level across slow walking speeds.

The measurement of vertical impulses from independent forelimb and hindlimb strides (Fig. 7B) suggests that giraffes maintain a forelimb to hindlimb vertical impulse distribution of 65:35 across a modest walking speed range. By this measure, giraffes are broadly similar to most other quadrupedal mammals, despite having a large (and long) mass of neck and head attached to the cranial thorax.

$\text{Impulse}_{\text{CC}}$ values are often different in quadrupeds' forelimbs and hindlimbs, owing to the specialised functions of these limbs in braking and propulsion (Griffin et al., 2004; Pandy et al., 1988). Our results indicate that propulsion in giraffes is shared between the forelimb and hindlimb. In contrast, braking impulses were significantly greater ($P<0.001$; Table S1) in the forelimb, indicating that the giraffe forelimb has a dominant role in decelerating the COM during steady-state locomotion, a feature that is shared by many other non-primate quadrupeds, including dogs, goats, elephants and grizzly bears (Griffin et al., 2004; Pandy et al., 1988; Ren et al., 2010; Shine et al., 2015).

Giraffe neck oscillation during walking is tied to stride frequency, whereby the neck oscillates twice through one walking stride period. We assessed the biomechanical importance of this oscillation by estimating the periodic tangential acceleration of the neck and its phase relative to the acceleration of the trunk. For this purpose, we modelled the neck and head as a massless hinged rod with a point mass of 80 kg at the distal end. The length of the rod (r) was equal to the radius of gyration of the neck–head system, assuming the simplified geometry of a uniform cylinder and an overall length of 1.5 m (Eqn 7). Kinematic data were then used as inputs to derive the tangential acceleration of the neck. In this model, the point mass oscillates around a starting angle (θ, measured from a vertical reference) with magnitude (q_0) and angular frequency (ω). q_0 was neck ROM/2 (measured from a vertical reference) and ω (rad s^{-1}) was dependent on the stride duration (Eqn 8). The sine oscillation was offset by i seconds to match the phase of the oscillation observed in experimental data. i was derived by fitting the neck angle in each trial to Eqn 9, using the 'fit' function in Matlab. ROM and ω were derived from the mean values from 46 trials (Table S5):

$$r = \frac{\text{neck length}}{\sqrt{3}}, \tag{7}$$

$$\omega = \frac{2\pi}{0.5 \times \text{stride duration}}. \tag{8}$$

Neck angle (q) at each time step (t) may then be modelled as follows:

$$q = q_0 \times \sin(\omega(t + i)) + \theta. \tag{9}$$

The goodness of fit of this model was checked for each trial, with a resulting mean±s.d. RMSE of 2.3±1.5 deg. The horizontal and vertical displacement of the neck (Fig. S1) at each time step was then expressed as:

$$\text{Horizontal displacement} = r \times \sin(q). \tag{10}$$

$$\text{Vertical displacement} = r \times \cos(q). \tag{11}$$

Eqns 10 and 11 were differentiated twice with respect to time, to derive the neck's acceleration at each time step. Peak neck accelerations were multiplied by neck mass to calculate horizontal and vertical tangential force. This model predicts that giraffes' peak vertical neck accelerations are low, with the resulting force equalling 1.2% of BW. Predicted peak horizontal accelerations are also modest, with a force of 0.8% BW (accounting for approximately 15% of peak GRF_{CC}). At faster speeds, we predict that neck tangential forces are greater, as the model predicts an increase to the square of stride frequency, and we independently observed an increase in neck ROM with walking speed (Fig. 2B).

The effect of the neck's tangential forces on the COM is dependent on the phase relationship between the neck and the trunk. We used the modelled neck accelerations and mean GRFs to calculate the phase relationship between the accelerations of the trunk and neck. Vertical and horizontal accelerations were evaluated separately. We assumed that the relationship between neck force (F_{neck}), trunk force (F_{trunk}) and COM of mass force (F_{COM}) was as follows:

$$F_{\text{trunk}} = F_{\text{COM}} - F_{\text{neck}}. \tag{12}$$

COM forces can be determined by summing all GRFs throughout the stride cycle. In this instance, a COM force time series was modelled by superimposing mean forelimb and hindlimb GRFs, temporally spaced using mean limb phase and duty factor. GRFs were summed to derive an estimation of F_{COM}. COM acceleration (A_{COM}) was calculated as:

$$A_{\text{COM}} = \frac{F_{\text{COM}}}{\text{BM}}, \tag{13}$$

where BM is body mass. The acceleration of the neck (A_{neck}) in the horizontal and vertical planes was calculated by double-differentiating the displacement of the neck's point mass (Fig. S1) with respect to time.

F_{neck} was derived as follows:

$$F_{\text{neck}} = A_{\text{neck}} \times 0.1\text{BM}. \tag{14}$$

F_{trunk} was derived from Eqn 12, and its acceleration (A_{trunk}) calculated assuming that its mass (also encompassing the limbs) was 0.9×BM.

Journal of Experimental Biology (2019) 222, jeb159277. doi:10.1242/jeb.159277

The magnitude of the acceleration due to gravity (9.81 m s^{-2}) was subtracted from the vertical components of acceleration.

The phase relationship between neck and trunk acceleration was calculated as the fraction of the stride between their time series' maxima or minima. A phase of 0% (i.e. in-phase oscillation) between neck and trunk acceleration would indicate that the COM (the sum of neck and trunk) experiences greater acceleration and velocity – and therefore greater kinetic energy – than the trunk alone. In this situation, the neck is a potential burden for the giraffe's walking gait. In contrast, a phase of 25% of the stride (i.e. out-of-phase oscillation) would indicate that COM acceleration and velocity are instead diminished by neck movement; this would indicate a mechanical energy-saving mechanism.

We found that horizontal neck acceleration in giraffes is largely out of phase with trunk acceleration, with a phase relationship of 23% (Fig. 8A). For example, as the trunk is decelerated during the beginning of stance, the mass of the neck accelerates in the opposite direction. In a global inertial frame, the neck therefore experiences little horizontal acceleration. This is likely to be a result of the neck's inertia and its degrees of freedom with the trunk. In effect, the horizontal motion of the neck is passively decoupled from the motion of the rest of the body. As a consequence, we expect that horizontal COM forces (measured as GRF_{CC}) are attenuated by neck motion. This may explain why we did not observe any trends between GRF_{CC} and walking speed.

A parallel may be drawn between the horizontal phase relationship of the giraffe and the modern 'Martini glass' riding style in horse racing. In this riding style, the jockey oscillates their body in the horizontal plane, out of phase with the horizontal oscillations of the horse's trunk, effectively decoupling themselves from the trunk's horizontal accelerations. The advantage of this riding style is that the horse does not have to accelerate or decelerate the rider in the horizontal plane, which may be otherwise detrimental to the horse's athletic performance (Pfau et al., 2009).

Table 2. Stride predictions according to dynamic similarity, and comparisons with giraffe experimental data, including prediction percentage error (PPE)

Parameter	Equation from Alexander and Jayes (1983)	Prediction at mean *Fr*	Mean experimental value	PPE
Relative stride length (stride length/shoulder height)	$y=2.4Fr^{0.34\pm0.1}$	0.89	1.13	21.3
Forelimb duty factor	$y=0.52Fr^{-0.14\pm0.05}$	0.78	0.72	−8.7
Hindlimb duty factor	$y=0.52Fr^{-0.18\pm0.08}$	0.88	0.69	−27.4

95% confidence intervals for the predictive exponents are included. *Fr*, Froude number.

We propose that giraffes may benefit from a similar mechanism, albeit at walking speeds.

The phase relationship between the vertical oscillations of the neck and trunk was 15% (Fig. 8B), similar to previous findings in giraffes (Loscher et al., 2016). This suggests that mechanical energy conservation is modest with respect to supporting the weight of the head and neck. As accelerations are predicted to increase with the square of stride frequency, the amount of limb work required to support the BW may place a constraint upon maximum walking speed. Given the increase in metabolic energy associated with swinging appendages beyond their natural frequency (Doke et al., 2005), neck inertia may be one factor that influences gait transition.

One limitation of the above modelling was the variable agreement between Eqn 9 and experimentally measured neck angles. A potential source of error was our method of motivating the giraffes using feedstuffs, which may have introduced artefactual variation in neck kinematics. We therefore verified the modelled neck–trunk

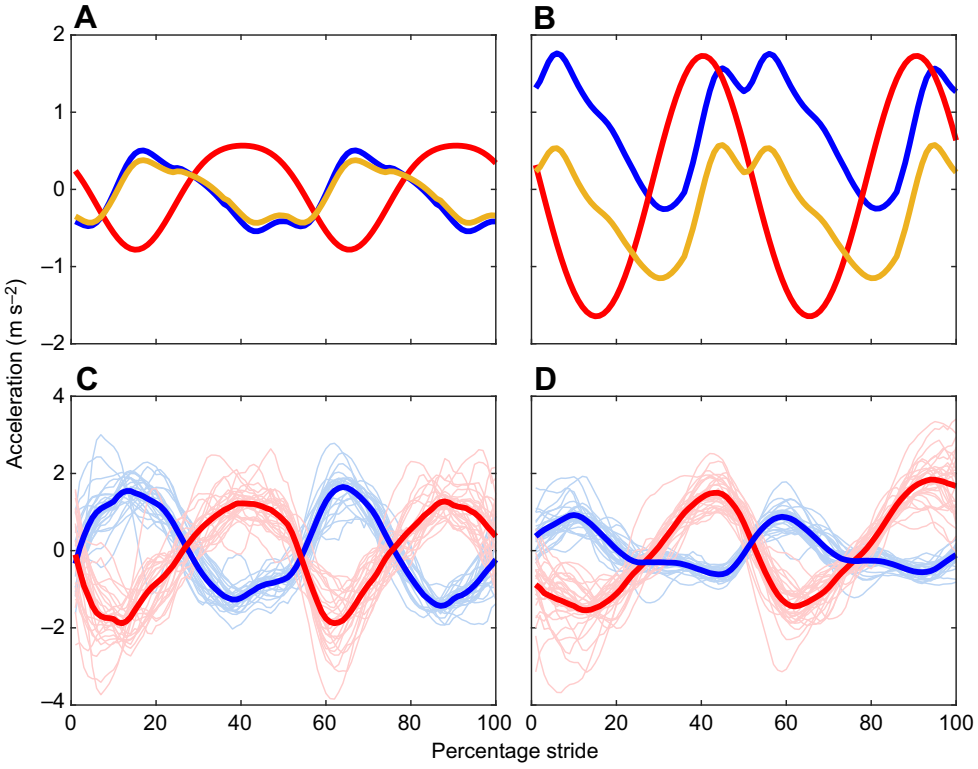

Fig. 8. Accelerations of neck, trunk and centre of mass during walking. Modelled horizontal (A) and vertical (B) tangential accelerations of the neck (red), trunk (blue) and COM (yellow). Neck acceleration was derived from mathematical modelling (Eqns 9, 10, 11) of neck oscillation; COM acceleration was derived from experimentally measured GRFs and limb phase; trunk acceleration was inferred from the subtraction of neck tangential force from COM force. Horizontal trunk and neck acceleration was timed with a phase of 23%, whilst vertical acceleration had a phase of 15%. The phasing of the modelled neck kinematics with COM forces was compared with empirical kinematic data by deriving horizontal (C) and vertical (D) accelerations of the virtual neck (red) and withers (blue) markers, with good agreement between phasing from the two methodologies. Thin lines show data from individual trials; thick lines represent mean values.

phase calculations against kinematic data. The phase relationship between the virtual withers and neck markers was calculated from each experimental trial (n=46). The mean horizontal phase from these trials (Fig. 8C) was 22±4.7% (mean±s.d.) and the mean vertical phase (Fig. 8D) was 17±4.0%; thus, there was good agreement between the modelled and empirical data.

The influence of neck posture and gravity on the mechanical cost of swinging the neck adds another layer of complexity to this system, as does the involvement of the nuchal ligament, which is likely to passively store and release elastic energy. A muscle-driven forward dynamics simulation would be a novel method of simulating the effect of stride frequency and neck posture on limb work.

Our signal-to-noise ratio was affected by the low range of speeds observed and the scatter induced by our experimental setup. During data collection, the giraffe keepers made efforts to encourage a wider range of speeds, but this resulted in poor subject compliance and (at best) excluded trial data. The observed speed range may therefore be viewed as being semi-selected by the giraffes. Our decision to use a sandy substrate on top of our force platform was made to address the logistical challenges that came with working in this environment. Whilst this inevitably introduced a degree of noise into our dataset, it also resulted in a larger number of trials than would have otherwise been possible. Our substrate setup means the results are subjectively more applicable to giraffes living in a naturalistic environment, compared with giraffes kept on hard surfaces.

We did not detect significant inter-subject variation in stride length or peak force. Although giraffe 3 had a history of overgrown forefeet, this does not appear to have affected the gait parameters. Despite this, we observed variation between giraffes in the symmetry of their forelimb GRF_{vert} profiles (Fig. 5C,D). Varying asymmetry was also evident from an additional (fourth) giraffe from an earlier study, walking at 0.027–0.14 *Fr*. These GRF data (Warner et al., 2013) were gathered under different experimental conditions to the present study, including hard substrate. In light of this, the asymmetrical GRF_{vert} profile of the forelimb appears to be a consistent feature of giraffe locomotion. We also observed intra-subject variation in the hindlimb GRF_{vert} profile (Fig. 5E,F). Within the same subject, the profile featured either two or three vertical peaks. The reason for this variability is unclear. Three-peaked GRF_{vert} profiles are also seen in elephants (Ren et al., 2010), so this may be a feature of extreme body mass or long limb length.

Linear regression of the Fourier coefficients offers mechanistic insight into how GRF_{vert} changes over the speed range. Each of the coefficients of the forelimbs increased significantly in magnitude with speed (Fig. 6), resulting in GRF_{vert} profiles with exaggerated peaks in late stance phase and lower mid-stance forces. This pattern of change is consistent with findings in walking adults and children, and has been linked to a stiff-limbed pendulum model of walking (Hubel and Usherwood, 2015).

It remains to be seen how much giraffes deviate from dynamic similarity when compared with other mammalian quadrupeds. Dynamic similarity (Alexander and Jayes, 1983) is directly related to geometric similarity, meaning animals that are geometrically similar will move in a dynamically similar fashion (where linear dimensions, time intervals and forces are related by constant factors) at equal dimensionless speed. A giraffe is not geometrically similar to a rhinoceros – giraffes have a metatarsal to femur length ratio of 1.4, compared with 0.33 in *Ceratotherium simum* (Garland and Janis, 1993) – but deviations from dynamic similarity may illustrate how the locomotor system in giraffes has become specialised. Any similarities should give us confidence when extrapolating biomechanical principles from other (cursorial) animals to giraffes, or even from giraffes to their extinct cousins (Basu et al., 2016). For example, giraffes' relative stride length at a *Fr* of 0.054 can be predicted using Alexander's power equations (table 2 of Alexander and Jayes, 1983) with a PPE of 21%, although PPE may be as low as 5% when the full range of dynamic similarity solutions are explored, using the models' confidence intervals. Duty factor yields similar levels of prediction errors (Table 2), and a limb phase of 0.14 is consistent with fig. 2 of Alexander and Jayes (1983) (when expressed in equivalent terms). A 70:14 gait (Fig. 3) is also found within the continuum of symmetrical gaits of other quadrupedal vertebrates (Hildebrand, 1989). In light of these similarities, we conclude that the walking gait of giraffes is not as functionally distinct as often stated.

We suggest that despite a suite of stark morphological specialisations, giraffes walk using the same mechanistic principles that underlie slow-speed walking in most other mammalian quadrupeds. This does not mean that the gait kinetics or kinematics of giraffes can simply be modelled from those of other animals. Rather, other models of quadrupedal locomotion can be used to generate testable hypotheses; for example, to test athletic performance at the more extreme ranges of ability in giraffes, or to explain more complex mechanisms (e.g. force, work and power at the level of the limb, joint or musculotendon units) used during walking.

Acknowledgements
We thank ZSL Whipsnade Zoo for allowing us to gather data from their giraffes, and to the staff (and giraffes) for their effort and patience during data collection. Thanks also to the staff and students of the Structure & Motion Laboratory for assisting with experiments; the RVC porters for carrying heavy things; to Luke Grinham for assistance with video analysis; to Jeff Rankin for his assistance in equipment troubleshooting; to Ruby Chang for statistical advice; and to Jim Usherwood and Jorn Cheney for helpful discussions. We acknowledge and thank two anonymous reviewers who improved this paper with their insightful comments.

Competing interests
The authors declare no competing or financial interests.

Author contributions
Conceptualization: C.B., A.M.W., J.R.H.; Methodology: C.B., A.M.W., J.R.H.; Software: C.B.; Validation: C.B.; Formal analysis: C.B.; Investigation: C.B.; Resources: C.B., A.M.W., J.R.H.; Data curation: C.B.; Writing - original draft: C.B.; Writing - review & editing: C.B., A.M.W., J.R.H.; Visualization: C.B.; Supervision: J.R.H.; Project administration: J.R.H.; Funding acquisition: J.R.H.

Funding
We thank the Natural Environment Research Council (NERC) for funding this research (PhD studentship for C.B.; grant no. NE/K004751/1 to J.R.H.).

Data availability
Ground reaction force data and associated stride parameters have been deposited in figshare: https://doi.org/10.6084/m9.figshare.7297778

Supplementary information
Supplementary information available online at
http://jeb.biologists.org/lookup/doi/10.1242/jeb.159277.supplemental

References
Alexander, R. M. N. and Jayes, A. S. (1980). Fourier analysis of forces exerted in walking and running. *J. Biomech.* **13**, 383-390.
Alexander, R. M. N. and Jayes, A. S. (1983). A dynamic similarity hypothesis for the gaits of quadrupedal mammals. *J. Zool.* **201**, 135-152.
Alexander, R. M. N., Langman, V. A. and Jayes, A. S. (1977). Fast locomotion of some African ungulates. *J. Zool.* **183**, 291-300.
Alexander, R. M. N., Maloiy, G. M. O., Hunter, B., Jayes, A. S. and Nturibi, J. (1979). Mechanical stresses in fast locomotion of buffalo (*Syncerus caffer*) and elephant (*Loxodonta africana*). *J. Zool.* **189**, 135-144.
Basu, C., Falkingham, P. L. and Hutchinson, J. R. (2016). The extinct, giant giraffid Sivatherium giganteum: skeletal reconstruction and body mass estimation. *Biol. Lett.* **12**.

Bates, K. T., Mannion, P. D., Falkingham, P. L., Brusatte, S. L., Hutchinson, J. R., Otero, A., Sellers, W. I., Sullivan, C., Stevens, K. A. and Allen, V. (2016). Temporal and phylogenetic evolution of the sauropod dinosaur body plan. *R. Soc. Open Sci.* **3**.

Benjamini, Y. and Hochberg, Y. (1995). Controlling the false discovery rate: a practical and powerful approach to multiple testing. *J. R. Stat. Soc. Ser. B* **57**, 289-300.

Bennett, M. B. (2001). Tetrapod walking and running. In *eLS*. John Wiley & Sons, Ltd.

Biewener, A. A. (1983). Allometry of quadrupedal locomotion: the scaling of duty factor, bone curvature and limb orientation to body size. *J. Exp. Biol.* **105**, 147-171.

Buchner, H. H. F., Savelberg, H. H. C. M., Schamhardt, H. C. and Barneveld, A. (1997). Inertial properties of Dutch Warmblood horses. *J. Biomech.* **30**, 653-658.

Cameron, E. Z. and du Toit, J. T. (2007). Winning by a neck: tall giraffes avoid competing with shorter browsers. *Am. Nat.* **169**, 130-135.

Crevier-Denoix, N., Robin, D., Pourcelot, P., Falala, S., Holden, L., Estoup, P., Desquilbet, L., Denoix, J. M. and Chateau, H. (2010). Ground reaction force and kinematic analysis of limb loading on two different beach sand tracks in harness trotters. *Equine Vet. J.* **42**, 544-551.

Dagg, A. I. (1962). The role of the neck in the movements of the giraffe. *J. Mammal.* **43**, 88-97.

Dagg, A. I. and Vos, A. D. (1968a). Fast gaits of pecoran species. *J. Zool.* **155**, 499-506.

Dagg, A. I. and Vos, A. D. (1968b). The walking gaits of some species of Pecora. *J. Zool.* **155**, 103-110.

Doke, J., Donelan, J. M. and Kuo, A. D. (2005). Mechanics and energetics of swinging the human leg. *J. Exp. Biol.* **208**, 439-445.

Garland, T. and Janis, C. M. (1993). Does metatarsal/femur ratio predict maximal running speed in cursorial mammals? *J. Zool.* **229**, 133-151.

Gatesy, S. M. and Biewener, A. A. (1991). Bipedal locomotion: effects of speed, size and limb posture in birds and humans. *J. Zool.* **224**, 127-147.

Griffin, T. M., Main, R. P. and Farley, C. T. (2004). Biomechanics of quadrupedal walking: how do four-legged animals achieve inverted pendulum-like movements? *J. Exp. Biol.* **207**, 3545-3558.

Hedrick, T. L. (2008). Software techniques for two- and three-dimensional kinematic measurements of biological and biomimetic systems. *Bioinspir. Biomim.* **3**, 034001.

Hildebrand, M. (1976). Analysis of tetrapod gaits: general considerations and symmetrical gaits. *Neural Control Locomot.* **18**, 203-206.

Hildebrand, M. (1989). The quadrupedal gaits of vertebrates. *Bioscience* **39**, 766-775.

Hubel, T. Y. and Usherwood, J. R. (2015). Children and adults minimise activated muscle volume by selecting gait parameters that balance gross mechanical power and work demands. *J. Exp. Biol.* **218**, 2830-2839.

Hudson, P. E., Corr, S. A. and Wilson, A. M. (2012). High speed galloping in the cheetah *(Acinonyx jubatus*) and the racing greyhound (*Canis familiaris*): spatio-temporal and kinetic characteristics. *J. Exp. Biol.* **215**, 2425-2434.

Hummel, J. (2006). Giraffe husbandry and feeding practices in Europe. Results of an EEP survey. 6th Congress of the European Association of Zoo and Wildlife Veterinarians, Budapest (Hungary), 24 May 2006 - 28 May 2006, 71-74.

Hutchinson, J. R., Schwerda, D., Famini, D. J., Dale, R. H., Fischer, M. S. and Kram, R. (2006). The locomotor kinematics of Asian and African elephants: changes with speed and size. *J. Exp. Biol.* **209**, 3812-3827.

Innis, A. C. (1958). The behaviour of the giraffe, Giraffa camelopardalis, in the eastern Transvaal. In *Proceedings of the Zoological Society of London*, Vol. 131, pp. 245-278. Wiley Online Library.

Kar, D., Issac, K. K. and Jayarajan, K. (2003). Gaits and energetics in terrestrial legged locomotion. *Mech. Mach. Theory* **38**, 355-366.

Lee, D. V., Bertram, J. E. and Todhunter, R. J. (1999). Acceleration and balance in trotting dogs. *J. Exp. Biol.* **202**, 3565-3573.

Loscher, D. M., Meyer, F., Kracht, K. and Nyakatura, J. A. (2016). Timing of head movements is consistent with energy minimization in walking ungulates. *Proc. R. Soc. B* **283**.

McMahon, T. A., Valiant, G. and Frederick, E. C. (1987). Groucho running. *J. Appl. Physiol.* **62**, 2326-2337.

Mitchell, G., Roberts, D., van Sittert, S. and Skinner, J. D. (2013). Growth patterns and masses of the heads and necks of male and female giraffes. *J. Zool.* **290**, 49-57.

Pandy, M. G., Kumar, V., Berme, N. and Waldron, K. J. (1988). The dynamics of quadrupedal locomotion. *J. Biomech. Eng.* **110**, 230-237.

Parkes, R. S. V. and Witte, T. H. (2015). The foot–surface interaction and its impact on musculoskeletal adaptation and injury risk in the horse. *Equine Vet. J.* **47**, 519-525.

Pfau, T., Spence, A., Starke, S., Ferrari, M. and Wilson, A. (2009). Modern riding style improves horse racing times. *Science* **325**, 289-289.

Pfau, T., Hinton, E., Whitehead, C., Wiktorowicz-Conroy, A. and Hutchinson, J. R. (2011). Temporal gait parameters in the alpaca and the evolution of pacing and trotting locomotion in the Camelidae. *J. Zool.* **283**, 193-202.

Raichlen, D. A., Pontzer, H., Shapiro, L. J. and Sockol, M. D. (2009). Understanding hind limb weight support in chimpanzees with implications for the evolution of primate locomotion. *Am. J. Phys. Anthropol.* **138**, 395-402.

Ren, L., Miller, C. E., Lair, R. and Hutchinson, J. R. (2010). Integration of biomechanical compliance, leverage, and power in elephant limbs. *Proc. Natl Acad. Sci. USA* **107**, 7078-7082.

Shine, C. L., Penberthy, S., Robbins, C. T., Nelson, O. L. and McGowan, C. P. (2015). Grizzly bear (Ursus arctos horribilis) locomotion: gaits and ground reaction forces. *J. Exp. Biol.* **218**, 3102-3109.

Simmons, R. E. and Scheepers, L. (1996). Winning by a neck: sexual selection in the evolution of giraffe. *Am. Nat.* **148**, 771-786.

Starke, S. D. and Clayton, H. M. (2015). A universal approach to determine footfall timings from kinematics of a single foot marker in hoofed animals. *PeerJ* **3**, e783.

Walker, A. M., Pfau, T., Channon, A. and Wilson, A. (2010). Assessment of dairy cow locomotion in a commercial farm setting: the effects of walking speed on ground reaction forces and temporal and linear stride characteristics. *Res. Vet. Sci.* **88**, 79-187.

Warner, S. E., Pickering, P., Panagiotopoulou, O., Pfau, T., Ren, L. and Hutchinson, J. R. (2013). Size-related changes in foot impact mechanics in hoofed mammals. *PLoS ONE* **8**, e54784.

Witte, T. H., Knill, K. and Wilson, A. (2004). Determination of peak vertical ground reaction force from duty factor in the horse (*Equus caballus*). *J. Exp. Biol.* **207**, 3639-3648.

Zajac, F. E. (1989). Muscle and tendon: properties, models, scaling, and application to biomechanics and motor control. *Crit. Rev. Biomed. Eng.* **17**, 359-411.